Very Large Spontaneous-Emission β Factors in Photonic-Crystal Waveguides

G. Lecamp, P. Lalanne, and J. P. Hugonin

Laboratoire Charles Fabry de l'Institut d'Optique, CNRS, Univ Paris-Sud, Campus Polytechnique, RD128, 91127 Palaiseau cedex, France

(Received 1 September 2006; published 11 July 2007)

Through a new rigorous Bloch-mode formalism, we theoretically study the generation of photons in single-row-defect photonic-crystal waveguides. In contrast with previous related works relying on a reinforcement of the spontaneous emission (SE) through microcavity effects, we explore situations for which the SE into radiation modes is reduced to a very low level while the SE into the guided mode is maintained at a level comparable to that in the bulk material. Remarkably large SE β factors in excess of 95% are obtained, and since no resonance effect is involved, this efficiency is achieved over a 40-nm-large spectral interval at $\lambda \approx 950$ nm.

DOI: 10.1103/PhysRevLett.99.023902 PACS numbers: 42.70.Qs, 41.20.Jb, 42.50.Pq

It has been recognized for some time that a new generation of optoelectronic devices like low-threshold lasers or single-photon sources can be drastically improved in terms of noise and speed modulation if their radiation pattern is highly directed toward a single mode and if the fraction of spontaneous emission (SE) coupled into this mode is made close to unity [1]. For low excitation, this fraction is defined as the SE coupling factor β. But in general, not all the radiation funnels into a single mode and a portion γ of the SE radiates out of this mode. This limitation has motivated the concept of 3D photonic-band-gap materials [2], which theoretically provides vanishing γ's. Nevertheless, in planar systems, only 2D photonic band gaps are achievable and up to now the main approach for increasing β has consisted in using the dynamic funneling of the photons (Purcell effect) provided by microcavities. Little is known on optical mechanisms for decreasing γ. In fact, such mechanisms rely on the suppression of the dipole-field coupling over all radiation modes and thereby touch difficult computational problems in electromagnetism.

In this Letter, we show that remarkably high β's can be achieved in photonic-crystal (PC) planar systems without any frequency-selective microcavity effect. We first present a general formalism for the light-emission calculation of a quantum dot (QD) in periodic waveguides. This derivation is motivated by the increasing use of PC waveguides for cavity quantum electrodynamics experiments [3] and nanocavity lasers [4]. Then we study the PC waveguide of Fig. 1(a) and design the line defect so as to minimize γ. While the total SE rate in the engineered structure remains comparable to that in the bulk, γ is reduced to such an extent that β factors in excess of 95% are observed for the two in-plane dipole orientations. Moreover, since the approach does not rely on any resonance effect, the efficient photon collection is achieved over a wide 40-nm spectral bandwidth at $\gamma \approx 950$ nm, releasing the restrictive atom-cavity spectral matching required in cavities.

In the electromagnetic description adopted here and in the weak coupling regime, the β factor of the PC waveguide can be predicted by calculating the classical photonic local density of states (LDOS) [5], and then by differentiating from the total field the relative weight of the guided and radiative contributions. To calculate the LDOS, one possible approach consists of using a finite computational window with perfectly matched layers (PMLs) in all directions [6]. For z-periodic waveguides, PMLs can be efficiently incorporated in the translational invariant x and y directions; see Fig. 1. However, the periodic z direction is more problematical. PML-like absorbing boundaries have been recently optimized for handling terminations in the periodic directions [7]; nevertheless, they break the periodicity and thus the source emission is inevitably spoiled by the backscattered light, especially for small group velocities. Hereafter, we overcome this theoretical difficulty by analytically handling the z direction [8]. Overall, with the analytical treatment and the PMLs, the new system shown in Fig. 1(b) can be rigorously treated on a finite transversal computational domain. Concretely, it means that the electromagnetic solutions of the two systems of Fig. 1 are identical inside the inner PML boundaries. Because of the presence of the PMLs, the new system is now dissipative. It supports an enumerable set (not a con-

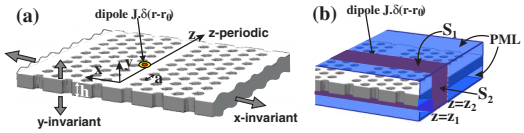

FIG. 1 (color online). (a) PC waveguide considered in this work and formed by removing a single row in a triangular lattice of air holes in a semiconductor membrane (thickness h) with air claddings. (b) Associated computational geometry obtained by surrounding the actual waveguide with PMLs (in blue) in the transverse translation-invariant directions. The dark purple part helps visualizing the surfaces S_1 and S_2. The PML thickness is not shown for the sake of clarity.

tinuum) of quantized modes that vanish at the outer PML boundaries and that can be numerically handled. Except for the truly guided mode, the modes depend on the specific implementation of the PMLs, they will be referred to as quasinormal Bloch modes (QNBMs). We will show that it is possible to define an orthogonality product for these modes and that the new system allows for a full treatment of the dipole-field coupling.

Potentially the forward-propagating QNBMs encompass a finite set of truly guided modes—the waveguide is assumed to be monomode hereafter and this mode will be denoted $\mathbf{\Phi}^{(1)} = [\mathbf{E}^{(1)}, \mathbf{H}^{(1)}]\exp(jk_1 z)$, with $\mathrm{Im}(k_1) = 0$—and an enumerable set $(m > 1)$ of leaky modes $\mathbf{\Phi}^{(m)} = [\mathbf{E}^{(m)}, \mathbf{H}^{(m)}]\exp(jk_m z)$, with $\mathrm{Im}(k_m) > 0$. The 6-component vectors $[\mathbf{E}^{(m)}, \mathbf{H}^{(m)}]$ are z-periodic functions of period a. Similarly, we denote by $\mathbf{\Phi}^{(-m)} = [\mathbf{E}^{(-m)}, \mathbf{H}^{(-m)}]\exp(-jk_m z)$ the associated backward-propagating modes. The total field $\mathbf{\Psi}(\mathbf{r})$ radiated by a Dirac dipole source $\mathbf{J}\delta(\mathbf{r}-\mathbf{r_0})$ can be expanded in terms of the complete set of outgoing QNBMs. For $z > z_0$ and $z < z_0$, we respectively have

$$\mathbf{\Psi}(\mathbf{r}) = \sum_{m>0} c_m^+ [\mathbf{E}^{(m)}(\mathbf{r}), \mathbf{H}^{(m)}(\mathbf{r})]\exp(jk_m z), \tag{1a}$$

$$\mathbf{\Psi}(\mathbf{r}) = \sum_{m>0} c_m^- [\mathbf{E}^{(-m)}(\mathbf{r}), \mathbf{H}^{(-m)}(\mathbf{r})]\exp(-jk_m z), \tag{1b}$$

where c_m^+ and c_m^- are the modal amplitude coefficients of the forward and backward QNBMs, respectively. To calculate these coefficients, we consider two solutions of Maxwell's equations for the same periodic-waveguide geometry, solution (1): $[\mathbf{E}_1, \mathbf{H}_1] = \mathbf{\Psi}(\mathbf{r})$ is the field in the presence of the Dirac source $J\delta(\mathbf{r}-\mathbf{r_0})$, and solution (2): $[\mathbf{E}_2, \mathbf{H}_2]$, a QNBM in the absence of any source. Referring to the Lorentz reciprocity theorem [9], one obtains $\oiint_S (\mathbf{E}_2 \times \mathbf{H}_1 - \mathbf{E}_1 \times \mathbf{H}_2)\cdot d\mathbf{S} = -\mathbf{E}_2(\mathbf{r}_0)\cdot\mathbf{J}$ for any closed surface S enclosing the source. We now apply the theorem to the closed surface formed by two waveguide cross sections, $z = z_1$ and $z = z_2$, and by the PML *outer-boundary* surfaces S_1 and S_2; see Fig. 1(b). Assuming that the surface-integral contribution is negligible at S_1 and S_2 (the electromagnetic fields fall off exponentially in the PMLs), one obtains by taking the field $\mathbf{\Psi}(\mathbf{r})$ of Eqs. (1a) and (1b) as solution (1), and $\mathbf{\Phi}^{(-p)}$ as solution (2),

$$c_p^+ \iint_{z=z_2} [\mathbf{E}^{(-p)}(\mathbf{r}) \times \mathbf{H}^{(p)}(\mathbf{r}) - \mathbf{E}^{(p)}(\mathbf{r}) \times \mathbf{H}^{(-p)}(\mathbf{r})]\cdot \mathbf{z}\, dS = -\mathbf{J}\cdot\mathbf{E}^{(-p)}(\mathbf{r}_0)\exp(-jk_p z_0). \tag{2a}$$

Similarly, using $\mathbf{\Phi}^{(p)}$ as solution (2), we have

$$c_p^- \iint_{z=z_1} [\mathbf{E}^{(-p)}(\mathbf{r}) \times \mathbf{H}^{(p)}(\mathbf{r}) - \mathbf{E}^{(p)}(\mathbf{r}) \times \mathbf{H}^{(-p)}(\mathbf{r})]\cdot \mathbf{z}\, dS = -\mathbf{J}\cdot\mathbf{E}^{(p)}(\mathbf{r}_0)\exp(jk_p z_0). \tag{2b}$$

To derive Eqs. (2a) and (2b), one has additionally used the orthogonality of QNBMs, which specifies that $\iint_A [\mathbf{E}^{(q)} \times \mathbf{H}^{(p)} - \mathbf{E}^{(p)} \times \mathbf{H}^{(q)}]\cdot \mathbf{z}\, dS$ is null if $q \neq -p$, for any waveguide cross section A. Importantly, note that the integrals over the cross section planes $z = z_1$ and $z = z_2$ in Eqs. (2a) and (2b) run over the entire waveguide cross sections, including the PML regions. Therefore the c_p's and the orthogonality relation are defined for the analytical continuations of the fields. In addition and consistently with the fact that the c_p's do not depend on the cross section, it is shown that the integrals on the left-hand sides of Eqs. (2a) and (2b) are equal. For the truly guided mode, $\mathbf{\Phi}^{(1)} = \mathbf{\Phi}^{(-1)*}$ so that Eqs. (2a) and (2b) further simplifies

$$c_1^- = (c_1^+)^* = -a(\mathbf{E}^{(1)}(\mathbf{r}_0)\cdot\mathbf{J})\exp(jk_1 z_0)/(4v_g\mathcal{E}_m), \tag{3}$$

with $2\mathcal{E}_m \int_{\mathrm{cell}} \varepsilon(\mathbf{r})|\mathbf{E}^{(1)}(\mathbf{r})|^2 d\mathbf{r}$ and v_g is the group velocity of $\mathbf{\Phi}^{(1)}$. In agreement with [8], the SE decay P_M into $\mathbf{\Phi}^{(1)}$ and $\mathbf{\Phi}^{(-1)}$ reads as $P_M(\mathbf{r}_0) = a|\mathbf{E}^{(1)}(\mathbf{r}_0)\cdot\mathbf{J}|^2/(8v_g\mathcal{E}_m)$ and scales as $(v_g)^{-1}$ [5].

As shown by Eqs. (2a) and (2b), the solution solely relies on the knowledge of the QNBMs. For calculating these modes, we use a Fourier modal method with PMLs in the x and y directions. The QNBMs are calculated as the eigenstates of the unit-cell transfer matrix; see details in [10]. Then, the c_m^+ and c_m^- coefficients are analytically calculated and, by using Eqs. (1a) and (1b), the field distribution is recovered everywhere. Thus the total SE rate is calculated as the Poynting-vector flux over a closed surface that is surrounding the source and that is fully enclosed inside the inner PML boundaries. By subtracting the guided-mode contribution P_M, the SE into radiation modes is obtained. We have performed various cross-checking tests by varying the PML thickness, the number of hole rows, and the Fourier space resolution. We estimate that the relative error on the computed data is $\pm 1\%$. Hereafter, we consider two in-plane dipole components and we assume that they are equally excited. For on-axis locations and because the z dipoles do not couple to the guided Bloch mode for symmetry reasons, only the continuum of radiation modes is excited with a SE rate denoted γ_z. For x dipoles, the SE rate is driven by both radiation (γ_x) and guided modes (P_M). Assuming random dipole orientations, the coupling factor β reads as $\beta = P_M/(P_M + \gamma_x + \gamma_z)$.

Figure 2 summarizes the main useful results predicted for a single-row-missing PC waveguide in a semiconductor $(n = 3.55)$ membrane in air, for three on-axis $(x_0 = 0, y_0 = -h/2)$ dipole locations, $z_0 = 0$, $a/4$, and $a/2$ [see Fig. 3(a) for the definition of z_0], and over the full-spectral interval of monomode operation from $a/\lambda = 0.243$ μm (band-edge cutoff) to $a/\lambda = 0.263$ μm (air-light line cutoff). All plots are normalized to the SE in the bulk material. The SE decay rate P_M into the guided modes [Fig. 2(b)] is essentially similar to that in the bulk material. As expected [5,8], it diverges as $1/v_g$ at the band edge where β asymptotically tends toward 1, except for the $z_0 = a/2$ dipole location (dotted black curve) for which the

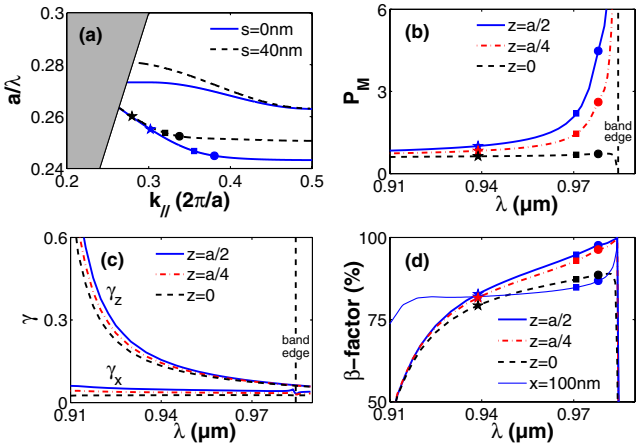

FIG. 2 (color online). Dipole radiation into a PC waveguide with $a = 240$ nm, $h = 0.75a$, and a hole radius of $0.29a$. (a) Dispersion diagram of the guided Bloch modes for $s = 0$ nm (solid blue curves) and for $s = 40$ nm (dashed black curves). (b) Normalized SE decay rate P_M into the fundamental Bloch modes. (c) Normalized SE decay rates into the radiation modes for the two in-plane dipole moment orientations. (d) Associated β factors. The thin solid blue curve is obtained for an off-axis dipole location ($x_0 = 100$ nm and $z_0 = a/2$). In all plots, circles, squares, and stars are reference marks locating the fundamental Bloch-mode group velocities equal to $c/20$, $c/10$, and $c/5$, respectively. From (b) to (d), three on-axis dipole locations, $z_0 = a/2$ (solid blue line), $a/4$ (dash-dotted red line), and 0 (dashed black line), are considered.

dipole-field coupling is null for symmetry reasons. Although the accompanied increase in the total SE rate is interesting in itself, we rather aim at exploring situations for which large β's are achieved by a decrease of γ alone and not by a spectrally selective LDOS enhancement like in microcavities. Relevant to this context are the small values of the SE rates γ_x and γ_z into the radiation states; see Fig. 2(c). γ_x is lower than 0.05 over the full frequency range, while γ_z is unfortunately very small only at large wavelengths, near the band-edge cutoff. Yet the β factor shown in Fig. 2(d) remains greater than 75% over a 50-nm

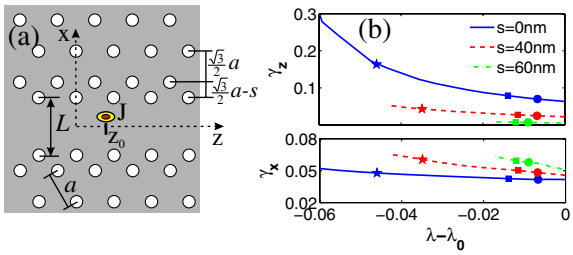

FIG. 3 (color online). Engineered PC waveguides for minimizing γ. (a) Definition of parameters s and L. (b) Effect of transversal shifts s on γ_x and γ_z for $L = \sqrt{3}a$ and $z_0 = a/2$. γ_x and γ_z are shown on the spectral domains of monomode operation for the PC waveguides, between the air-light line cutoff and the band-edge cutoff λ_0. Circles, squares, and stars as in Fig. 2.

spectral range, which already represents a much better performance than that achieved in classical dielectric z-invariant waveguides [11]. We have also performed calculations for off-axis dipole locations; it turns out that the SE rate into radiation modes remains rather low [γ_x and γ_z are similar to the on-axis case of Fig. 2(c)]. The x-dipole SE rate, P_M, into the guided mode decreases since the dipole-field coupling is weakened by transverse shifts or misalignments [Eq. (3)], but this lowering is roughly compensated by the existence of some z-dipole SE into this same guided mode. Overall, it results that the β factor remains above 75%, as shown by the thin solid curve in Fig. 2(d) obtained for $z_0 = 0$ and $x_0 = 100$ nm.

Actually, the drop of β at small wavelengths in Fig. 2(d) is due to the relatively high SE rate of the z dipole in radiation modes, $\gamma_z \approx 10\gamma_x$. It is well known that the SE of a dipole in the vicinity of a semiconductor-air interface oscillates as a function of the dipole-interface distance. For semiconductor membranes, the cavity effect due to two interfaces results in a minimal radiation-mode excitation for a membrane thickness equal to $\approx \lambda/2n$ [1], thus motivating the choice of a $h = 0.75a$ membrane thickness for the calculations and in earlier experimental works [3,4]. Applying the same idea to the x direction of the PC waveguide, we are facing a much stronger interaction because of the high reflectivity ($|r|^2 \approx 97\%$) at the PC boundaries [12]. We believe that this band-gap guidance is responsible for the lower γ_z values obtained with PC waveguides in comparison to those obtained for air-semiconductor wires, the latter suffering from weak reflections ($|r|^2 \approx 30\%$) at the interfaces in the two transversal directions.

Intuitively, two parameters, denoted by s and L in Fig. 3(a), allow one to monitor the amplitude and the retardation of the light reflected at the PC mirror: a shift s of the two inner first hole rows of the waveguide mainly reinforces the amplitude of the reflected light [12], while the defect width L controls the retardation effect. Although such a classical picture applied at a subwavelength scale is only approximate, it paves the way to control the vacuum-field radiation-mode coupling. Indeed we have performed calculations for the SE rates in the radiation modes and it turns out that the lateral shift s can largely impact γ_z. In Fig. 3(b), we show the trends observed by tuning s for $L = a\sqrt{3}$, similar results being obtained for other L values. As s increases, γ_x remains low and γ_z is reduced. But the downside is a decrease of the available wavelength range of monomode operation, which moves from 60 nm for $s = 0$ nm to less than 20 nm for $s = 60$ nm. In Fig. 4(b) (solid blue curve), we have plotted the spectral dependence of β for $s = 40$ nm, a geometry offering a good compromise. β remains higher than 88% over the 40-nm spectral range.

So far we have considered the β factor into two fundamental, counterpropagating modes. Yet photon emission into a single mode is highly desirable for applications and

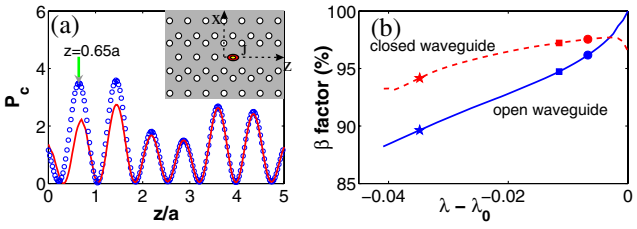

FIG. 4 (color online). Broadband photon emission into a single guided mode $\mathbf{\Phi}^{(1)}$ for the semiclosed geometry (inset). (a) SE decay rate P_c into $\mathbf{\Phi}^{(1)}$ for $a/\lambda = 0.255$, $s = 40$ nm, and $L = \sqrt{3}a$. Solid red curve: predictions of Eq. (4). Blue circles: data calculated with the fully vectorial formalism. (b) β factor of the open (solid blue curve) and semiclosed (dashed red curve) geometries for the engineered waveguide ($s = 40$ nm). The blue curve is obtained for $z_0 = a/2$, and the red curve for $z_0 = 0.65a$. Circles, squares, and stars as in Fig. 2.

can be simply achieved by closing an extremity of the waveguide by a semi-infinite Bragg mirror, as shown in the inset of Fig. 4(a). The β factor of the semiclosed geometry can be directly deduced from the previous results provided that one neglects the feedback coupling between the dipole and the radiation QNBMs excited by the dipole and backreflected by the mirror. Within this approximation, the SE decay rate P_c into $\mathbf{\Phi}^{(1)}$ is simply given by

$$P_c = |c_m^+(z_0) + rc_m^-(z_0)\exp(j2k_1z_0)|^2, \qquad (4)$$

where r is the modal reflectivity coefficient of $\mathbf{\Phi}^{(-1)}$ into $\mathbf{\Phi}^{(1)}$ ($|r|^2 \approx 98\%$) [12]. For $a/\lambda = 0.255$ ($v_g = c/8$), the dependence of P_c with the dipole location z_0 is shown in Fig. 4(a) with the solid red curve. P_c exhibits a quasiperiodic modulation with the dipole-mirror distance, which results from the interplay between the backscattered-mode phase matching (preponderant periodicity $2\pi/k_1$) and the dipole-Bloch-mode coupling coefficients $c_m^+(z_0)$ and $c_m^-(z_0)$ (periodicity a). The model predictions (solid red curve) well reproduce the numerical data (blue circles) obtained with the theoretical formalism, the difference vanishing as the impact of radiation QNBMs decreases by tunnelling, i.e., as z_0 increases. For efficient broadband single mode emission, the dipole location $z_0 = 0.65a$, marked with a green arrow in Fig. 4(a), is highly valuable since it offers constructive backscattering interferences of $\mathbf{\Phi}^{(1)}$ strengthened by a positive contribution of the radiation QNBMs. Using the theoretical formalism, we have calculated the β factor of the semiclosed geometry for this dipole location. The results are shown in Fig. 4(b) with the dotted red curve [13]. Quite remarkably, the β factor exceeds 95% over a 40-nm bandwidth, a value comparable with the inhomogeneous broadening of QD array emission lines.

In conclusion, we have shown that a very low coupling into the radiation modes is achievable in PC waveguides and that it allows a highly efficient funneling of light into a single mode over a large spectral range. This broadband operation releases the atom-cavity spectral matching required with resonators [14] and thus increases device yield. Moreover, by closing the engineered waveguide on both sides, very-high single-photon extraction efficiencies can be achieved without relying on a strong Purcell effect and thus operation at cryogenic temperatures can be considered. Furthermore, small γ's are important since large β enhancements driven by Purcell factor alone are always limited by the spectral width of the QD transition.

[1] T. Baba *et al.*, IEEE J. Quantum Electron. **27**, 1347 (1991).

[2] E. Yablonovitch, Phys. Rev. Lett. **58**, 2059 (1987).

[3] A. Kress *et al.*, Phys. Rev. B **71**, 241304(R) (2005); S. Laurent *et al.*, Appl. Phys. Lett. **87**, 163107 (2005); D. Englund *et al.*, Phys. Rev. Lett. **95**, 013904 (2005); W. H. Chang *et al.*, Phys. Rev. Lett. **96**, 117401 (2006).

[4] H. Y. Ryu *et al.* Appl. Phys. Lett. **84**, 1067 (2004); S. Strauf *et al.*, Phys. Rev. Lett. **96**, 127404 (2006); H. Altug, D. Englund, and J. Vuckovic, Nature Phys. **2**, 484 (2006).

[5] R. C. McPhedran *et al.*, Phys. Rev. E **69**, 016609 (2004).

[6] Here, we adopt the viewpoint of W. C. Chew and W. H. Weedon, Microw. Opt. Technol. Lett. **7**, 599 (1994). A PML in a given direction, say the α direction, is seen as a complex coordinate transform that virtually allows one to rigorously satisfy the outgoing wave conditions of a semi-infinite open α-invariant system into a finite computational window with vanishing fields at the outer boundary.

[7] A. R. Weily *et al.*, Microw. Opt. Technol. Lett. **40**, 1 (2004).

[8] An analytic treatment in the z direction of periodic waveguides has been recently used through a photonic Green-tensor formalism; see S. Hughes,Opt. Lett. **29**, 2659 (2004). However, in this previous work, only emission into the bounded Bloch mode is obtained. The approach adopted here additionally allows one to handle the coupling into the radiation Bloch modes, which is crucial in the present context.

[9] A. W. Snyder and J. D. Love, *Optical Waveguide Theory* (Chapman and Hall, New York, 1983). In contrast with the normal Bloch modes used in [8], the QNBMs are not orthogonal in the sense of the Poynting vector ($E \times H^*$ product) because of the PMLs. However, they indeed obey the unconjugate general form of orthogonality with $E \times H$ product.

[10] P. Lalanne, IEEE J. Quantum Electron. **38**, 800 (2002); E. Silberstein *et al.*, J. Opt. Soc. Am. A **18**, 2865 (2001).

[11] For instance, for semiconductor ($n = 3.5$) wires in air, β peaks at a value of 65% for a square geometry with a lateral size of $0.7\lambda/n$; see details in G. Lecamp *et al.*, Proc. SPIE-Int. Soc. Opt. Eng. **6195**, 61 950E (2006).

[12] C. Sauvan, P. Lalanne, and J. P. Hugonin, Phys. Rev. B **71**, 165118 (2005).

[13] As $v_g \to 0$, β does not tend towards 1 as it does for the open case; in fact, $\beta \to 0$. This is a consequence of the mode degeneracy ($\mathbf{\Phi}^{(-1)} = \mathbf{\Phi}^{(1)}$) at the Brillouin band edge and of the unitary modal reflectivity, all resulting in a null emission into $\mathbf{\Phi}^{(1)}$.

[14] A. Badolato *et al.*, Science **308**, 1158 (2005).